Biochimica et Biophysica Acta 1840 (2014) 1882–1891

Contents lists available at ScienceDirect

Biochimica et Biophysica Acta

journal homepage: www.elsevier.com/locate/bbagen

Thiol oxidation is crucial in the desensitization of the mitochondrial F_1F_O-ATPase to oligomycin and other macrolide antibiotics

Salvatore Nesci, Vittoria Ventrella, Fabiana Trombetti, Maurizio Pirini, Alessandra Pagliarani *

Department of Veterinary Medical Sciences, University of Bologna, via Tolara di Sopra 50, 40064 Ozzano Emilia, Bologna, Italy

ARTICLE INFO

Article history:
Received 17 October 2013
Received in revised form 12 December 2013
Accepted 2 January 2014
Available online 9 January 2014

Keywords:
Mitochondrial F_1F_O-ATPase
Uncompetitive inhibition
Oligomycin
Macrolide binding region
Thiol oxidation
Tributyltin

ABSTRACT

Background: The macrolide antibiotics oligomycin, venturicidin and bafilomycin, sharing the polyketide ring and differing in the deoxysugar moiety, are known to block the transmembrane ion channel of ion-pumping ATPases; oligomycins are selective inhibitors of mitochondrial ATP synthases.
Methods: The inhibition mechanism of macrolides was explored on swine heart mitochondrial F_1F_O-ATPase by kinetic analyses. The amphiphilic membrane toxicant tributyltin (TBT) and the thiol reducing agent dithioerythritol (DTE) were used to elucidate the nature of the macrolide–enzyme interaction.
Results: When individually tested, the macrolide antibiotics acted as uncompetitive inhibitors of the ATPase activity. Binary mixtures of macrolide inhibitors I_1 and I_2 pointed out a non-exclusive mechanism, indicating that each macrolide binds to its binding site on the enzyme. When co-present, the two macrolides acted synergistically in the formed quaternary complex (ESI_1I_2), thus mutually strengthening the enzyme inhibition. The enzyme inhibition by macrolides displaying a shared mechanism was dose-dependently reduced by TBT $\geq$ 1 μM. The TBT-driven enzyme desensitization was reversed by DTE.
Conclusions: The macrolides tested share uncompetitive inhibition mechanism by binding to a specific site in a common macrolide-binding region of F_O. The oxidation of highly conserved thiols in the ATP synthase *c*-ring of F_O weakens the interaction between the enzyme and the macrolides. The native macrolide-inhibited enzyme conformation can be restored by reducing crucial thiols oxidized by TBT.
General significance: The findings, by elucidating the macrolide inhibitory mechanism on F_O, indirectly cast light on the F_1F_O torque generation involving crucial amino acid residues and may address drug design and antimicrobial therapy.

1. Introduction

The mitochondrial F_1F_O-ATPase (EC 3.6.3.14) is a bi-powered enzymatic engine that exploits the transmembrane proton motive force Δp to clockwise rotate the membrane portion F_O, which channels H^+ and drives ATP synthesis from ADP and inorganic phosphate (P_i) by the hydrophilic catalytic sector F_1 through a torque generation mechanism. Conversely, through a counterclockwise rotation driven by ATP hydrolysis by F_1, the same enzyme complex converts the Gibbs free energy of hydrolysis in uphill proton transport through F_O, thus re-energizing mitochondria [1–3]. The bi-functional capability of the mitochondrial enzyme complex, a unique example of chemo-mechanical coupling in biological systems, is long known to be specifically inhibited by oligomycins (OLIGs) [4]. Accordingly, OLIG inhibition has been widely exploited to study the ATPase/synthase functionality in eukaryotic cells. Conversely OLIG, generally produced by *Streptomyces diastatochromogenes* and other *Streptomyces* species [5] as a mixture of structurally closely related compounds, is ineffective in bacterial F_1F_O-ATPase [6]. OLIG belongs to the polyketide class of macrolide antibiotics whose basic structure consists of polymers of ketide units, featured by a macrocyclic lactone ring bound to one or more deoxy-sugars. Some natural macrolides, such as apoptolidin and ossamycin produced by *Nocardiopsis* and various *Streptomyces* strains, are also known as potent inhibitors of F_O. Apparently, the macrolide ring confers the inhibition power, while the deoxysugar moiety is not crucial for ATPase inhibition [7]. After 50 years of studies, the OLIG binding site has been localized on F_O and precisely on the *c* subunits, which by forming a sort of cylindrical palisade constitutes the *c*-ring, a key element in the torque generation mechanism [2]. The *c*-subunit number, constant for a given species but variable among species, determines the *c*-ring size, in turn related to the bioenergetic efficiency, being small rings associated with low bioenergetic cost of ATP. This advantageous condition is apparently favored from an evolutionary standpoint [1,8,9]. Proton flux through the *c*-ring involves a carboxyl group which, approximately at the midpoint of each C-terminal α-helix, transfers protons by switching from the proton-locked conformation to the deprotonated open conformation [10]. From a close insight, OLIG, by binding to two adjacent *c*-subunits, would shield this carboxyl residue, block proton flux and inhibit the F_1F_O-ATPase/synthase activities [11]. The OLIG molecular arrangement

* Corresponding author. Tel.: +39 0512097017; fax: +39 0512097037.
E-mail address: alessandra.pagliarani@unibo.it (A. Pagliarani).

0304-4165/$ – see front matter © 2014 Elsevier B.V. All rights reserved.
http://dx.doi.org/10.1016/j.bbagen.2014.01.008

in the *c*-ring is thought to be shared by other macrolide antibiotics such as venturicidin (VENT) and bafilomycin (BAF) and to constitute the molecular basis of the F_1F_O complex inhibition. VENT strongly inhibited H^+-translocation and both ATP synthesis and hydrolysis in mitochondrial and in bacterial F_1F_O-ATPases [6]. BAF selectively inhibited V-type ATPases by a similar mechanism to that of eukaryotic F_1F_O-ATPase inhibition by OLIG [12,13]. Since the *c*-rings in the F- and V-ATPases are thought to stem from a common ancestor [14], the possibility that the two enzyme rotary complexes contain a similar antibiotic binding site seems not remote [12].

Antibiotic drug resistance can be achieved by a variety of mechanisms. Accordingly, the events involved in the mitochondrial F_1F_O-ATPase sensitivity loss to natural compounds such as OLIG, can be related to structural changes, in turn involving mitochondrial bioenergetics [15]. Interactions of macrolide antibiotics with the F_1F_O complex are an emerging field, up to now poorly explored [11]. Accordingly, by investigating through a kinetic approach the mutual behavior of OLIG, VENT and BAF in the mitochondrial F_1F_O-ATPase inhibition and the mechanisms of enzyme desensitization to these macrolide inhibitors, we primarily aimed at casting light on the antibiotic binding sites within F_O and on the energy transduction mechanisms involved in ATP synthesis. However, the results can also provide useful information for drug design and to exploit natural compounds as new therapeutic agents.

2. Materials and methods

2.1. Chemicals

Na_2ATP, oligomycin (a mixture of oligomycins A, B and C, in the proportion 64:15:17 respectively), tri-*n*-butyl chloride (TBT), 1,4-dithioerythritol (DTE) and 5,5′-dithiobis(2-nitrobenzoic acid) (DTNB) were of the highest purity available and obtained from Sigma–Aldrich (Milan, Italy). Venturicidin A and bafilomycin B_1 were of the highest purity available and obtained from Vinci-Biochem (Vinci, Italy). All other chemicals were reagent grade. Protein Assay kit II was purchased by Bio-Rad (Milan, Italy). Quartz double distilled water was used for all reagent solutions.

2.2. Preparation of the mitochondrial fractions

Swine hearts (*Sus scrofa domesticus*) were collected at a local abattoir and transported to the lab within 2 h in ice buckets at 0–4 °C. After removal of fat and blood clots as much as possible, approximately 30–40 g of heart tissue were rinsed in ice-cold washing Tris–HCl buffer (medium A) consisting of 0.25 M sucrose, 10 mM Tris(hydroxymethyl)-aminomethane (Tris), pH 7.4 and finely chopped into fine pieces with scissors. Each preparation was made from one heart. Once rinsed, tissues were gently dried on blotting paper and weighted. Then tissues were homogenized in the homogenizing buffer (medium B) consisting of 0.25 mM sucrose, 10 mM Tris, 0.2 mM EDTA (free acid), 0.5 mg/mL BSA, pH 7.4 with HCl. After a preliminary gentle break up by Ultraturrax T25, the tissue was carefully homogenized by a motor-driven Teflon pestle homogenizer (Braun Melsungen Type 853202) at 450 rpm with 5 up-and-down strokes. The mitochondrial fraction was then obtained by stepwise centrifugation (Sorvall RC2-B, rotor SS34) [16]. Briefly, the homogenate was centrifuged at 1000 *g* for 5 min, thus yielding a supernatant and a pellet. The pellet was re-homogenized under the same conditions of the first homogenization and re-centrifuged at 1000 *g* for 5 min. The gathered supernatants from these two centrifugations, filtered through four cotton gauze layers, were centrifuged at 10,500 *g* for 10 min to yield the raw mitochondrial pellet. The raw pellet was resuspended in medium A and further centrifuged at 10,500 *g* for 10 min to obtain the final mitochondrial pellet. The latter was resuspended by gentle stirring using a Teflon Potter Elvejehm homogenizer in a small volume of medium A, thus obtaining a protein concentration of 20–25 mg/mL. All steps were carried out at 0–4 °C. The protein concentration was determined according to the colorimetric method of Bradford [17] by Bio-Rad Protein Assay kit II with bovine serum albumin (BSA) as standard. The mitochondrial preparations were then stored in liquid nitrogen until the evaluation of ATPase activities.

2.3. Assay of the Mg-ATPase activity

The thawed mitochondrial fractions were immediately used for the Mg-ATPase activity assays. The capability of enzymatic ATP hydrolysis was assayed in a reaction medium (1 mL) containing 75 mM ethanolammine–HCl buffer pH 8.9, 6.0 mM Na_2ATP, 2.0 mM $MgCl_2$ and 0.15 mg mitochondrial protein. After 5 min at 30 °C, the reaction, carried out at 30 °C, was started by the addition of the substrate ATP and stopped after 5 min by the addition of 1 mL of ice-cold 15% (v/v) aqueous solution of trichloroacetic acid. Once the reaction was stopped, vials were centrifuged for 15 min at 5000 rpm (ALC 4225 Centrifuge). In the supernatant, the concentration of inorganic phosphate (P_i) hydrolyzed by known amounts of mitochondrial protein, which is an indirect measure of ATPase activity, was spectrophotometrically evaluated according to Fiske and Subbarow [18].

In all experiments the ATPase activity was calculated as μmoles Pi mg protein^{-1} h^{-1}. The data represent the mean ± SD (shown as vertical bars in the figures) of at least three replicates carried out on distinct tissue preparations.

2.4. Preincubation procedures

In selected experiments, to favor incorporation of the compounds within the mitochondrial membranes and avoid the direct interference between different reagents, enzymatic assays were carried out on mitochondria preincubated in vials for 30 min on ice with the compounds to be tested. Accordingly, the preincubation of mitochondria with selected TBT doses aimed at ensuring TBT incorporation within the membranes and at evaluating the effect of the thiol reagent dithioerythritol (DTE), ruling out a direct interaction between DTE and TBT. In detail, mitochondria were preincubated with 4 μL DMSO (control) or 4 μL of appropriate TBT solutions in DMSO to yield the final 35 μM TBT concentrations in the reaction system. To prevent possible chemical interactions between TBT and DTE, 100 μM DTE were added in the TBT-preincubated mitochondrial suspensions only when were acclimated at 30 °C. After this incubation time, the ATPase reaction was carried out as described in the previous section. The DTE concentrations were previously tested [19].

2.5. Kinetic analyses

Kinetic studies on the mutual interactions between two inhibitors (double inhibitors) of the same enzyme activity (mitochondrial ATPase) (Segel, 1975) were carried out to cast light on the possible binding site of macrolide antibiotics. In all kinetic analyses the enzyme specific activity was taken as the expression of the reaction rate (v).

The mechanism of the enzyme inhibition by OLIG, VENT and BAF was explored by the aid of the graphical methods of Dixon [20] and Cornish-Bowden [21] which complement one another.

A series of parallel lines at the different ATP concentrations tested is typical of uncompetitive inhibition. In this case, according to the Dixon equation:

$$\frac{1}{v} = \frac{1}{K_i' V_{max}}[I] + \frac{1}{V_{max}}\left(1 + \frac{K_m}{[S]}\right) \quad \text{(I)}$$

the slope corresponds to $1/K'iV_{max}$, where $K'i$ is the dissociation constant of the enzyme–inhibitor–substrate complex (*EIS*), and the intercept on the y axis corresponds to $(1 + K_m/[S])V_{max}{}^{-1}$.

According to the Cornish–Bowden equation:

$$\frac{S}{v} = \frac{[S]}{K_i' V_{max}}[I] + \frac{K_m + [S]}{V_{max}} \quad \text{(II)}$$

if the straight lines intersect above the x axis, namely in the y positive half-plane, the compound tested behaves as uncompetitive inhibitor [20]. In this case the abscissa of the intersection point corresponds to $-K'i$, while the ordinate corresponds to K_m/V_{max} [21].

The inhibition mechanism of the three antibiotics under study was further investigated by testing binary mixtures of inhibitors, namely by plotting $1/v$ vs. $[I_1]$ at different fixed $[I_2]$ and constant $[S]$ to build Dixon plots [22]. This experimental approach aimed at eliciting possible interactions between the compounds under study in their binding to the mitochondrial complex. Thus, on considering OLIG, VENT and BAF as three mitochondrial ATPase inhibitors (I_1, I_2, I_3), the enzyme activity was evaluated in the presence of increasing concentrations of the macrolide I_1 at fixed concentrations of the macrolide I_2 and at 6 mM ATP. The protocol described for I_1 and I_2 was also applied by testing the binary combinations $I_1 + I_3$ and $I_2 + I_3$. According to this diagnostic test, the simultaneous enzyme inhibition by the two inhibitors I_1 and I_2 fits Eq. (III) for synergistic uncompetitive inhibitors:

$$\frac{1}{v} = \frac{1}{K_{i1}' V_{max}}\left(1 + \frac{[I_2]}{\alpha K_{i2}'}\right)[I_1] + \frac{1}{V_{max}}\left(1 + \frac{K_s}{[S]} + \frac{[I_2]}{K_{i2}'}\right). \quad \text{(III)}$$

This situation implies that I_1 and I_2 simultaneously combine with the enzyme–ATP complex.

By fitting data according to Eq. (III), namely $1/v$ as a function of $[I_1]$, the abscissa of the point of intersection of the two straight lines obtained in the presence and absence of I_2 corresponds to $-\alpha K'i_1$, while the ordinate is $1/V_{max}(1-\alpha + K_S/[S])$.

The value of $\alpha K'i_2$ was calculated from the slopes of the straight lines obtained in the presence (slope $I_1 + I_2$) and in the absence of I_2 (slope I_1) according to the following relation:

$$\alpha K_{i2}' = \frac{[I_2]}{\frac{slope I_1 + I_2}{slope I_1} - 1}. \quad \text{(IV)}$$

For each macrolide antibiotic, once obtained the values of $\alpha K'i$ from the Dixon plot of mutual interactions between two inhibitors and of $K'i$ from the Cornish–Bowden plot, the interaction constant (α) was directly obtained from the ratio:

$$\alpha = \frac{\alpha K_i'}{K_i'}. \quad \text{(V)}$$

In all plots, the correlation coefficients were always higher than 0.97, thus confirming the linearity of the graphs.

The IC_{50} values of the antibiotics under study were graphically interpolated from the inhibition curves of the mitochondrial ATPase, which followed the equation for a single exponential decay with offset, namely to a non-zero value:

$$y = A_0 \cdot e^{-kx} + offset. \quad \text{(VI)}$$

The enzyme activity data showing the decrease in the Mg-ATPase sensitivity to macrolide antibiotics in the presence of TBT fitted to the exponential equation:

$$y = A_0 \cdot e^{-kx}. \quad \text{(VII)}$$

In both equations A_0 corresponds to the enzyme activity value in the absence of inhibitor, namely to the intercept of the plots with y axis, while k is a constant related to the curve gradient.

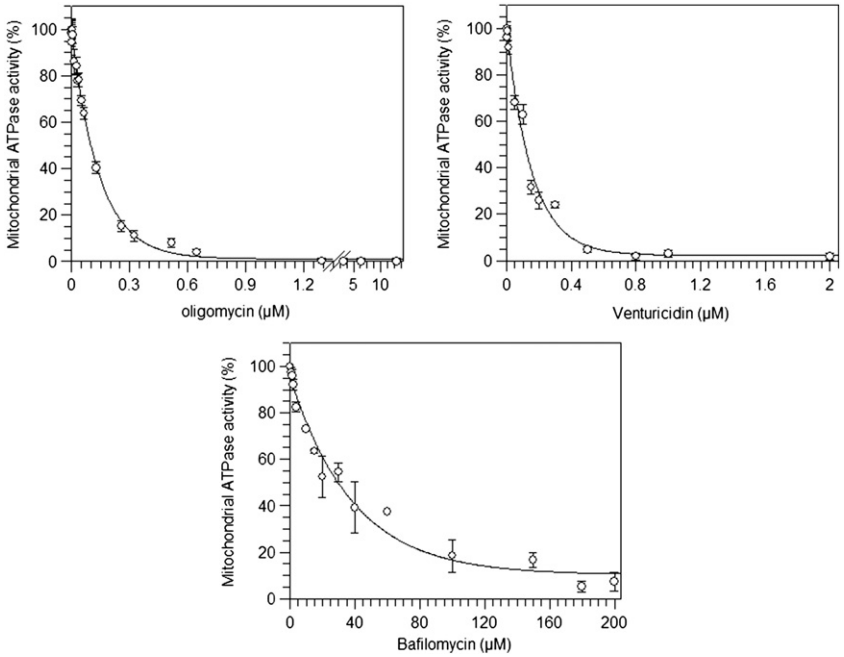

Fig. 1. Mitochondrial ATPase inhibition by oligomycin, venturicidin and bafilomycin. The enzyme activities are expressed as percentage of the enzyme activity detected in the absence of oligomycin, venturicidin and bafilomycin, respectively. Each point represents the mean ± SD (vertical bars) from 3 determinations carried out on distinct pools.

2.6. Quantitative evaluation of SH groups

Mitochondrial thiol concentrations under various experimental conditions were colorimetrically quantified by Ellman's reagent [23]. This widely used method is based on the capability of 5,5′-dithiobis(2-nitrobenzoic acid) (DTNB) to react with free thiol groups by forming disulphide bonds with thionitrobenzoic acid (TNB). Since the ratio of protein thiol to TNB formed is 1:1, TNB formation was used to assess the number of thiols present [24]. After the addition of 15% v/v trichloroacetic acid solution (250 μL/0.15 mg protein) to precipitate proteins, the mitochondrial suspension was centrifuged at 12,000 *g* for 5 min at 4 °C, the supernatant removed and the mitochondrial pellet carefully resuspended with potter Eppendorf pestle. Then, 400 μL of DTNB solution containing 0.5 M phosphate buffer (KH_2PO_4/K_2HPO_4, pH 7.4), 0.2 mM DTNB, 5 mM EDTA, was added to the suspension and incubated for 15 min at 4 °C. Absorbance at 412 nm (maximum TNB absorption wavelength) of the supernatant from a second centrifugation at 12,000 *g* for 5 min at 4 °C was read on a Perkin-Elmer lambda 45 spectrophotometer. Thiol groups in mitochondria were quantitatively evaluated by interpolating the absorbance values in a calibration curve built by employing known cysteine concentrations as –SH standard. In each experiment set, data were expressed as percentage of the 100% free –SH groups in TBT free medium which was considered as control [25].

2.7. Statistics

The data represent the mean ± SD (shown as vertical bars in the figures) of the number of experiments reported in figure captions and table legends. In each experimental set, the analyses were carried out on different pools of animals. The differences between data obtained in the presence and in the absence of the inhibitors to be tested in the ATPase reaction mixtures were evaluated by one way ANOVA followed by Dunnett's test or Students–Newman–Keuls' test, when *F* values indicated significance ($P \leq 0.05$).

3. Results

3.1. Inhibition of the mitochondrial Mg-ATPase activity

As shown in Fig. 1, the sensitivity of mitochondrial ATPase activity to OLIG, VENT and BAF was evaluated by testing increasing concentrations

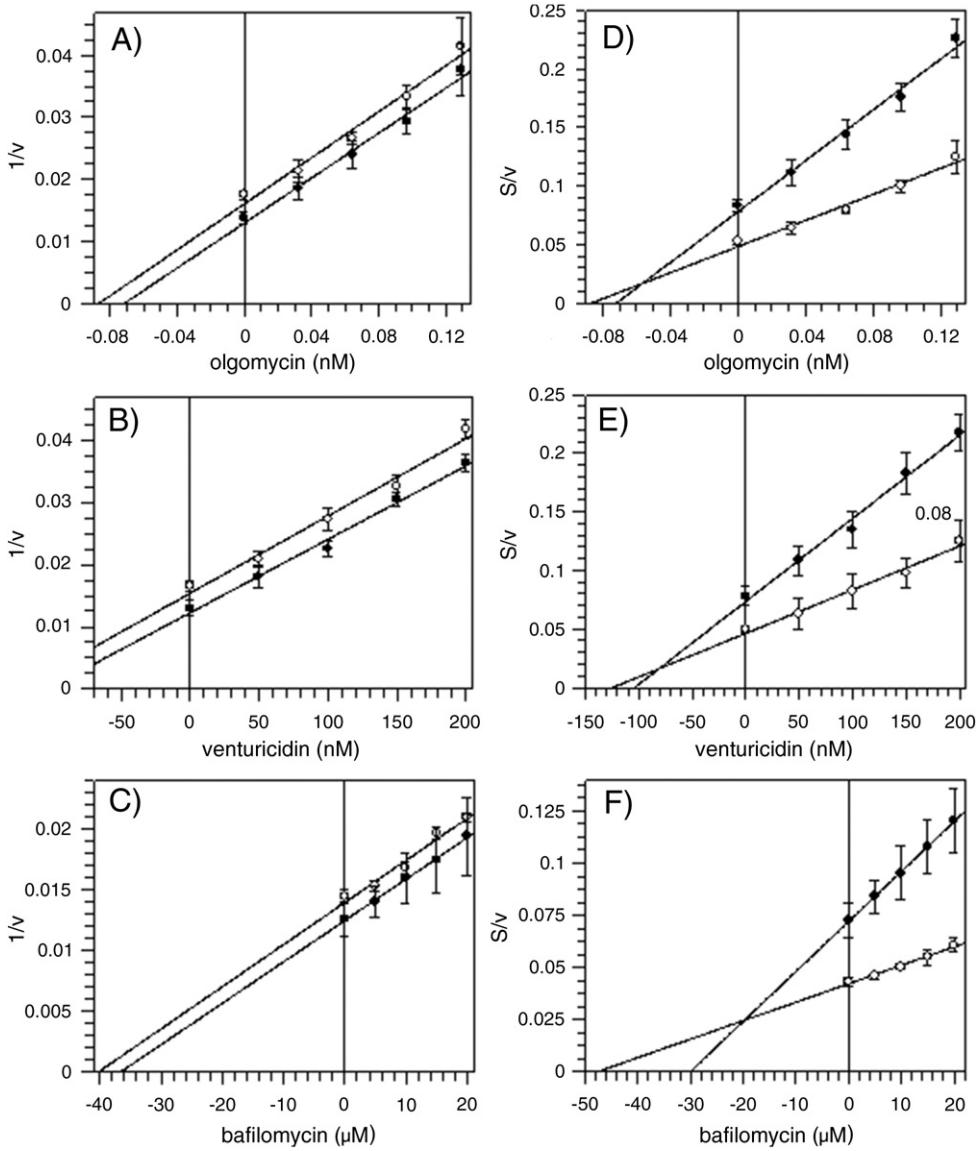

Fig. 2. Mitochondrial ATPase inhibition by oligomycin, venturicidin and bafilomycin. Dixon (A, B, C) and Cornish–Bowden (D, E, F) plots drawn at 6.0 (●) and 3.0 (○) mM ATP as detailed in Section 2.5. All points represent the mean ± SD (vertical bars) of four distinct experiments carried out on distinct pools. Data were fitted to straight lines by linear regression ($R > 0.97$).

Table 1
IC_{50} and $K'i$ values for the mitochondrial ATPase inhibition by oligomycin (OLIG), venturicidin (VENT) and bafilomycin (BAF).

	IC_{50} (μM)	$K'i$ (μM)
OLIG	0.092 ± 0.003 a	0.056 ± 0.004 a
VENT	0.105 ± 0.005 a	0.081 ± 0.003 a
BAF	28.7 ± 2.8 b	22.1 ± 4.0 b

Data are the mean ± SD from 3 determinations on distinct pools. Different letters indicate significantly different values between the mitochondrial ATPase activity ($P \leq 0.05$), evaluated by one-way ANOVA, followed by Students–Newman–Keuls' test.

Table 2
$\alpha K'i$ values (μM) for the quaternary complex ESI_1I_2 by the non-exclusive inhibitors oligomycin (OLIG), venturicidin (VENT) and bafilomycin (BAF) as binary combinations.

ES I_2 + I_1	$\alpha K'i_1$	Fig. 3 panel
ES VENT + OLIG	0.058	A
ES BAF + OLIG	0.021	B
ES BAF + VENT	0.017	C
ES I_1 + I_2	$\alpha K'i_2$	
ES OLIG + VENT	0.083	A
ES OLIG + BAF	14.0	B
ES VENT + BAF	1.5	C

$\alpha K'i_1$ and $\alpha K'i_2$ refer to the reaction equilibria of Fig. 4; $\alpha K'i_1$ values were graphically obtained from the Dixon plots in the named Fig. 3 panel; $\alpha K'i_2$ values were calculated by Eq. (IV) from the Dixon plot slopes in the named Fig. 3 panel.

of the compounds under study individually. The maximal enzyme inhibition was attained at different macrolide concentrations, namely 100% inhibition at approximately 1.3 μM OLIG (Fig. 1A), 98% at 1.0 μM VENT (Fig. 1B) and 90% at 180 μM BAF (Fig. 1C).

The inhibition mechanism was further explored by testing increasing concentrations of OLIG, VENT and BAF at the two constant concentrations of 3 and 6 mM ATP. The resulting Dixon plots consisted of two parallel straight lines, one for each of the two employed ATP concentrations (Fig. 2 A,B,C). By building the Cornish–Bowden plots (Fig. 2 D,E,F), the two straight lines obtained intersected above the *x* axis, namely in the *y* positive half-plane. Therefore both Dixon and Cornish–Bowden plots, which provide complementary information, were consistent with uncompetitive inhibition mechanism [22] for all the compounds tested.

The dose–response profiles (Fig. 1), the IC_{50} values, graphically interpolated, and the $K'i$ values, obtained from the Cornish–Bowden plots (Table 1), lead to think that the inhibition efficiency followed the order OLIG ≥ VENT >> > BAF.

3.2. Multiple inhibition analysis

Once assessed that all the macrolide tested behaved as uncompetitive inhibitors of the F_1F_O-ATPase, the graphical method detailed in the Section 2.5. was applied to discriminate if two macrolide antibiotics interacted with the mitochondrial complex, and presumptively with F_O, by the same site or by different sites. This method, by exploring the effect of binary mixtures of inhibitors of the same enzyme activity to build the corresponding Dixon plots, also provides a tool to calculate the interaction constant (α) between two compounds under study in the formation of the enzyme–substrate–inhibitor/s complex [22]. By plotting the reciprocal of the ATPase activity as a function of increasing OLIG concentrations in the presence and in the absence of fixed VENT concentrations (Fig. 3A), two straight lines intersecting above the *x* axis were obtained. The graphically obtained $\alpha K'i_1$ value is the product of the interaction constant α per dissociation constant ($K'i_1$) of OLIG from the enzyme–substrate–venturicidin complex (*ES* VENT) (Table 2). Similarly, by employing adequate binary mixtures of macrolides, namely increasing [OLIG] and constant [BAF] (Fig. 3B), and increasing [VENT] and constant [BAF] (Fig. 3C), the graphically obtained $\alpha K'i$ values are related to the dissociation constants of the *ES* BAF OLIG complex and of the *ES* BAF VENT complex, respectively. Accordingly, the two values could be taken respectively as indicators of OLIG (Fig. 3B) and VENT capability

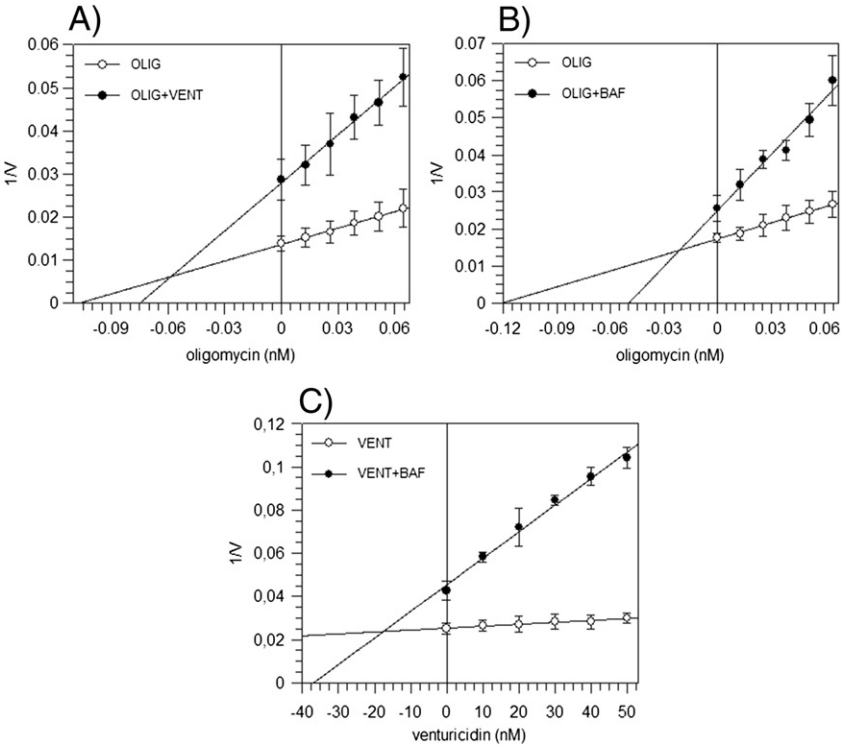

Fig. 3. Multiple inhibitor analysis by Dixon plots for the F_1F_O-ATPase inhibition by oligomycin (OLIG), venturicidin (VENT) and bafilomycin (BAF). ATPase assays were carried out in the presence of 6 mM ATP and A) OLIG (○) or OLIG + 125 nM VENT (●); B) OLIG (○) or OLIG + 35 μM BAF (●); C) VENT (○) or VENT + 35 μM BAF (●). All points represent the mean ± SD (vertical bars) of three distinct experiments carried out on distinct pools. ($R > 0.97$).

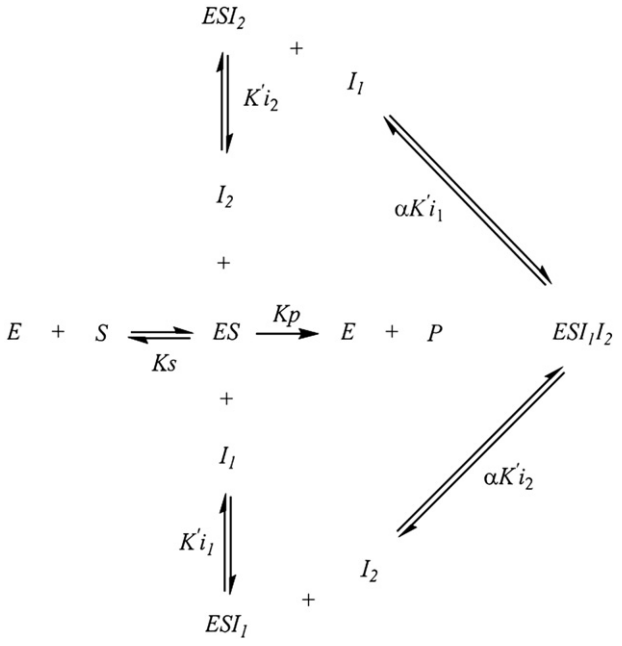

Fig. 4. Reactions involved in the synergistic uncompetitive inhibition by the non-exclusive inhibitors I_1 and I_2 [22].

Table 3
Interaction constants (α) between OLIG, VENT and BAF, as non-exclusive inhibitors I_1 and I_2 in the ESI_1I_2 complex formation.

	OLIG	VENT	BAF
OLIG	–	1.0 (b)	0.6 (b)
VENT	1.0 (a)	–	0.1 (b)
BAF	0.4 (a)	0.2 (a)	–

(a) Calculated from the $\alpha K'i$ value graphically obtained; (b) calculated from Eq. (IV). I_1 and I_2 represent two out of three macrolides according to the inhibitor combination tested.

(Fig. 3C) of binding to the *ES* BAF ternary complex to form a quaternary complex enclosing two inhibitors, according to the pattern depicted in Fig. 4. In other words in all these plots, which are typical of enzyme inhibition by two different inhibitors which act simultaneously on the same enzyme [22], the product $\alpha K'i_1$ is somehow inversely related to the strength by which the inhibitor assayed at varied concentrations (I_1) binds to the formed quaternary complex ESI_2I_1 in the reaction system. As depicted in Fig. 4, since the $\alpha K'i_1$ value contains the dissociation constant, the higher is $\alpha K'i_1$ value the less stable is the ESI_2I_1 complex, showing that I_1 is poorly efficient in binding to ESI_2. Assumed that the macrolides I_1 and I_2 can exchange their priority roles, namely first I_1 binds to *ES* and I_2 binds to the already formed ESI_1 complex (Fig. 4), by exploiting Eq. (IV), the $\alpha K'i_2$ values were calculated from the corresponding plots in Fig. 3 using Eq. (IV). $\alpha K'i_2$ values can be taken as a measure of the tendency of I_2 to dissociate from ESI_1I_2, to yield the ternary complex ESI_1. Consistently, high $\alpha K'i_2$ value means that I_2 has a poor tendency to bind to ESI_1. All $\alpha K'i_1$ and $\alpha K'i_2$ values are shown in Table 2.

At this point the results suggest that, when two of the three macrolides under study co-occur in the reaction system (Fig. 3), they behave as uncompetitive inhibitors (I_1 and I_2) and can both combine with the enzyme to form the ESI_1I_2 complex. For two given macrolides, this complex can be formed by two alternative pathways, depending on which inhibitor binds first to the *ES* complex (Fig. 4). The $\alpha K'i_1$ and $\alpha K'i_2$ values (Table 2), can be helpful to trace the apparently easier pathway for each macrolide couple to yield the quaternary complex, based on the dissociation constants of the two reactions leading to the ESI_1I_2 complex.

Furthermore the interaction constant (α) between the two different inhibitors bound to the enzyme, obtained from the ratio between $\alpha K'i$ and $K'i$ (Eq. (V)), (Table 3), can help to cast light on the possible reciprocal interference between two macrolides in their binding to *ES*. Accordingly, when $\alpha = 1$, the two inhibitors bind independently from each other to yield the ESI_1I_2 complex. In this case $K'i_1$ equals $K'i_2$, namely the stability of the quaternary complex is independent of the binding sequence of the two inhibitors. Conversely, if $0 < \alpha < 1$, the two inhibitors mutually favor each other (positive attraction) in the ESI_1I_2 formation [22]. According to α values (Table 3) OLIG and VENT bound

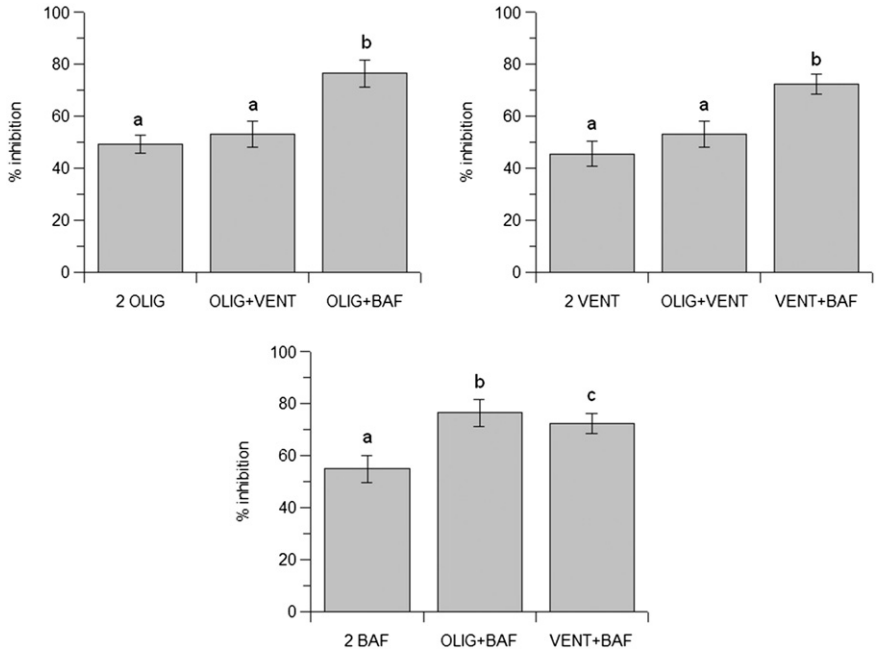

Fig. 5. Mitochondrial ATPase inhibition by oligomycin (OLIG), venturicidin (VENT) and bafilomycin (BAF) and by macrolide binary mixtures. The inhibition percentage (%) was calculated with respect to the ATPase activity in the absence of macrolides. Inhibitor concentrations equal to $2\times K'i$ were individually tested, namely 112.4 nM OLIG, 162.2 nM VENT and 44.2 μM BAF. Inhibitor concentrations equal to $K'i$ were employed in the binary mixtures, namely 56.2 nM OLIG, 81.1 nM VENT and 22.1 μM BAF. Data are the mean ± SD (vertical bars) of three different experiments carried out on distinct pools. In each panel different letters indicate significantly different values ($P \leq 0.05$) evaluated by one-way ANOVA followed by Dunnett's test.

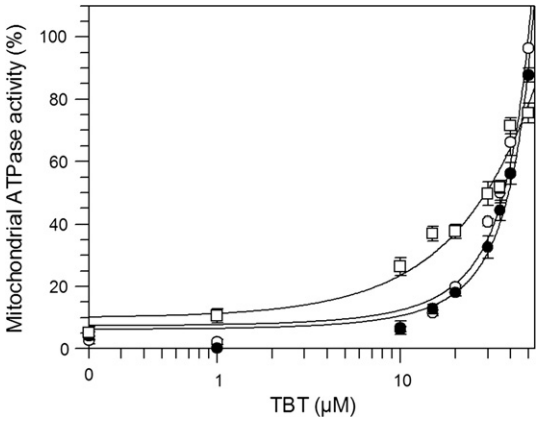

Fig. 6. Effect of TBT on the F_1F_O-ATPase sensitivity to oligomycin (OLIG), venturicidin (VENT) and bafilomycin (BAF). The Mg-ATPase activity, assayed in the presence of 1.3 μM OLIG (○), 1.0 μM VENT (●) and 180.0 μM BAF (□) and increasing concentrations of TBT, is expressed as percentage (%) of the enzyme activity detected in absence of inhibitors. Each point represents the mean ± SD (vertical bars) of three distinct experiments.

independently, while OLIG and BAF as well as VENT and BAF strengthened their binding to the *ES* complex.

The synergistic behavior of the uncompetitive inhibitors under study was explored by comparing the effect of binary mixtures of macrolides with the individual effect of either of the two macrolides at a twofold concentration than that in the mixture [22]. In this diagnostic test, the concentrations of I_1 and I_2 in each binary mixture should correspond to their respective $K'i$ values (Table 1). Accordingly, if the enzyme activity inhibition percentage produced by $[I_1] = K'i_1$ plus $[I_2] = K'i_2$ was higher than that detected at $[I_1] = 2\ K'i_1$ or $[I_2] = 2\ K'i_2$, as it happened under all the conditions tested (Fig. 5), the two inhibitors acted synergistically, namely their binary mixtures produced a higher-than-additive effect. Furthermore, it seems worthwhile noticing that under all the conditions tested, the BAF occurrence in the binary mixture strongly potentiated the effect of the other co-present macrolide.

3.3. Thiol involvement in macrolide inhibition

Since the mitochondrial ATPase sensitivity to OLIG and other F_O inhibitors was found to be decreased by the synthetic xenobiotic TBT at ≥ 1 μM concentration [15], the enzyme activity was evaluated in the presence of 1.3 μM OLIG, 1.0 μM VENT and 180 μM BAF and increasing TBT concentrations to check any possible variation in the enzyme susceptibility to the macrolide inhibitors promoted by TBT (Fig. 6). The three selected macrolide concentrations lay in the range producing the maximal ATPase activity inhibition (Fig. 1). As shown in Fig. 6, increasing TBT micromolar concentrations promoted an exponential increase in the ATPase activity refractory to the compounds tested. Thus, since the macrolide-insensitive ATPase activity attained 100% of the enzyme activity at the highest TBT concentration tested, the enzyme inhibition by 1.3 μM OLIG, 1.0 μM VENT and 180 μM BAF was completely removed. The exponential curves showed similar gradients for OLIG (0.0525 ± 0.0043) and VENT (0.0537 ± 0.0033), both steeper than that of BAF (0.0298 ± 0.0046). These results clearly showed that TBT dose-dependently desensitized the ATPase activity to the three macrolides tested and that the desensitizer efficiency of TBT was especially striking for the two powerful inhibitors OLIG and VENT.

The F_1F_O-ATPase desensitization by 35 μM TBT, a concentration which caused a 50% increase in the macrolide-insensitive enzyme activity, was further investigated by carrying out assays on TBT-preincubated mitochondria in the presence and in the absence of the reducing agent DTE. As detailed in the Section 2.4, this protocol aimed at favoring TBT incorporation within the mitochondrial membranes and at avoiding any possible direct interaction between DTE and TBT. In Fig. 7 the height of the histograms is indicative of the ATPase activity under the various experimental conditions tested. In the absence of TBT the sensitivity of mitochondrial ATPase to 1.3 μM OLIG (Fig. 7A), 1.0 μM VENT (Fig. 7B) and 180 μM BAF (Fig. 7C), expressed as a residual ATPase activity in the presence of these macrolide inhibiting concentrations, was unaffected by 100 μM DTE. As expected, in TBT-preincubated mitochondria the sensitivity of the enzyme complex to the three antibiotics tested decreased by approximately 50%, as shown by the significant ATPase

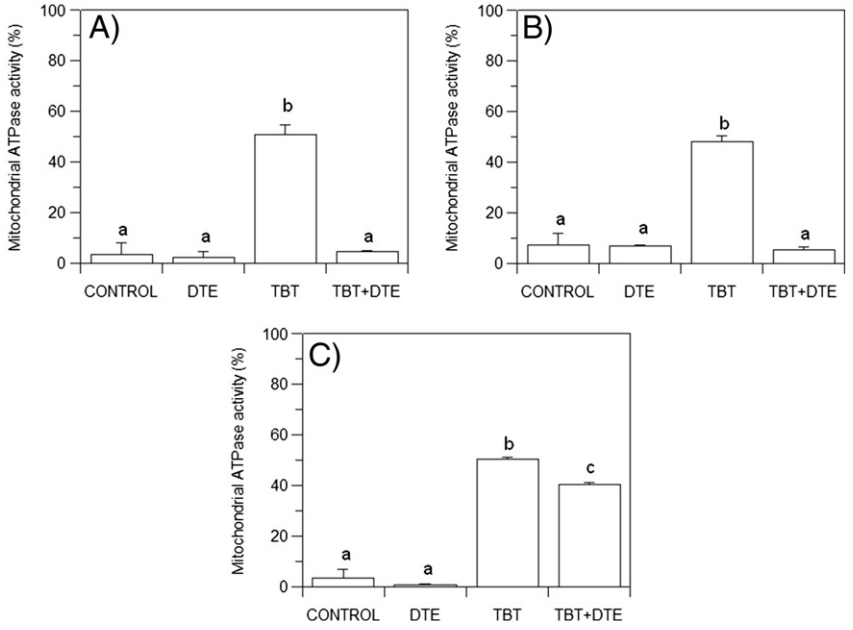

Fig. 7. DTE-promoted recovery of the F_1F_O-ATPase sensitivity to oligomycin (OLIG), venturicidin (VENT) and bafilomycin (BAF). The mitochondrial ATPase activity, expressed as percentage (%) of the enzyme activity in the absence of macrolides, was assayed in a reaction medium containing 0.15 mg mitochondrial protein and, according to the condition to be tested, 1.3 μM OLIG (A), 1.0 μM VENT (B), 180.0 μM BAF (C), 100 μM DTE, 35 μM TBT, as written under the histograms. Control: the reaction medium contained DMSO-preincubated mitochondria plus OLIG (A), VENT (B) and BAF (C). The data are the mean ± SD (vertical bars) of three different experiments carried out on distinct pools. In each panel the different letters indicate significantly different values ($P \leq 0.05$) evaluated by one-way ANOVA followed by Student–Newman–Keuls' test.

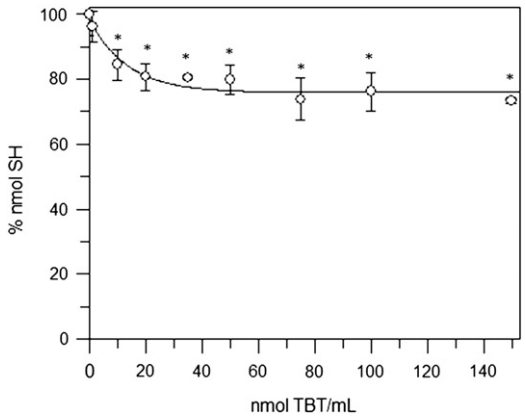

Fig. 8. Available free –SH groups in mitochondrial proteins at increasing TBT concentrations. Data are expressed as percentage (%) of –SH groups in control mitochondria (in the absence of TBT). Each value is the mean ± SD (vertical bars) of three experiments carried out on mitochondria from different preparations. The asterisks indicate significantly different values from the control at $P \leq 0.05$. One-way ANOVA, Dunnett's test.

activity rise with respect to untreated mitochondria (Fig. 7, panels A, B and C, respectively). The enzyme desensitization by TBT was almost completely removed by DTE, whose addition reduced the ATPase activity in the presence of OLIG (A) and VENT (B) to nearly undetectable levels. Apparently DTE was less efficient in the removal of the ATPase activity inhibition by BAF (C), since the enzyme activity recovery in TBT-preincubated mitochondria was only 20% reduced by DTE.

The TBT interaction with mitochondrial thiol groups was confirmed by the quantitative evaluation of the free (unbound) –SH groups in mitochondria by Ellman's reagent, in the absence and presence of increasing TBT concentrations. In a reaction system containing 0.15 mg mitochondrial protein, a significant decrease in free –SH groups with respect to the control (corresponding to 100% free thiols) was shown from 10 nmol TBT/mL onwards. The number of free thiol groups dose-dependently decreased up to attain the maximal reduction of 26% with respect to the control at 75 nmol TBT/mL, roughly corresponding to 500 nmoles TBT per mg of mitochondrial protein (Fig. 8).

4. Discussion

Due to its central role in cell bioenergetics and survival, the mitochondrial F_1F_O-ATPase/synthase represents an intriguing molecular tool to elicit wanted and unwanted effects of drugs. Up to now this enzyme complex has been increasingly shown to be targeted by a variety of therapeutic molecules [26]. Among them, F_O inhibitors are especially interesting because they can be exploited as a tool to cast light on some still poorly elucidated aspects of the F_1F_O-ATPase/synthase mechanism of torque generation. From the first discovery, the F_1F_O complex has gathered variegated definitions from "A splendid molecular machine" [27] to "…one of the wonders of the molecular world, it is an enzyme, a molecular motor, an ion pump, and another molecular motor all wrapped together in one amazing nanoscale machine" [28]. Among F_O inhibitors, the natural macrolide antibiotics here investigated, namely OLIG, VENT and BAF, represent a fascinating example of how structural differences between related macrolides confer different inhibition potency through a similar inhibition mechanism. The similarity of the three structures under study only lies in the polyketide backbone (Fig. 9) claimed to be crucial for the enzyme inhibition [7] and probably also for the same uncompetitive mechanism. Undoubtedly the interaction of OLIG with the enzyme complex is the most investigated and known. OLIG precisely binds on two adjacent *c* subunits of F_O (shown as *c1* and *c2* in Fig. S1) [11] and, by covering the *c1* binding site

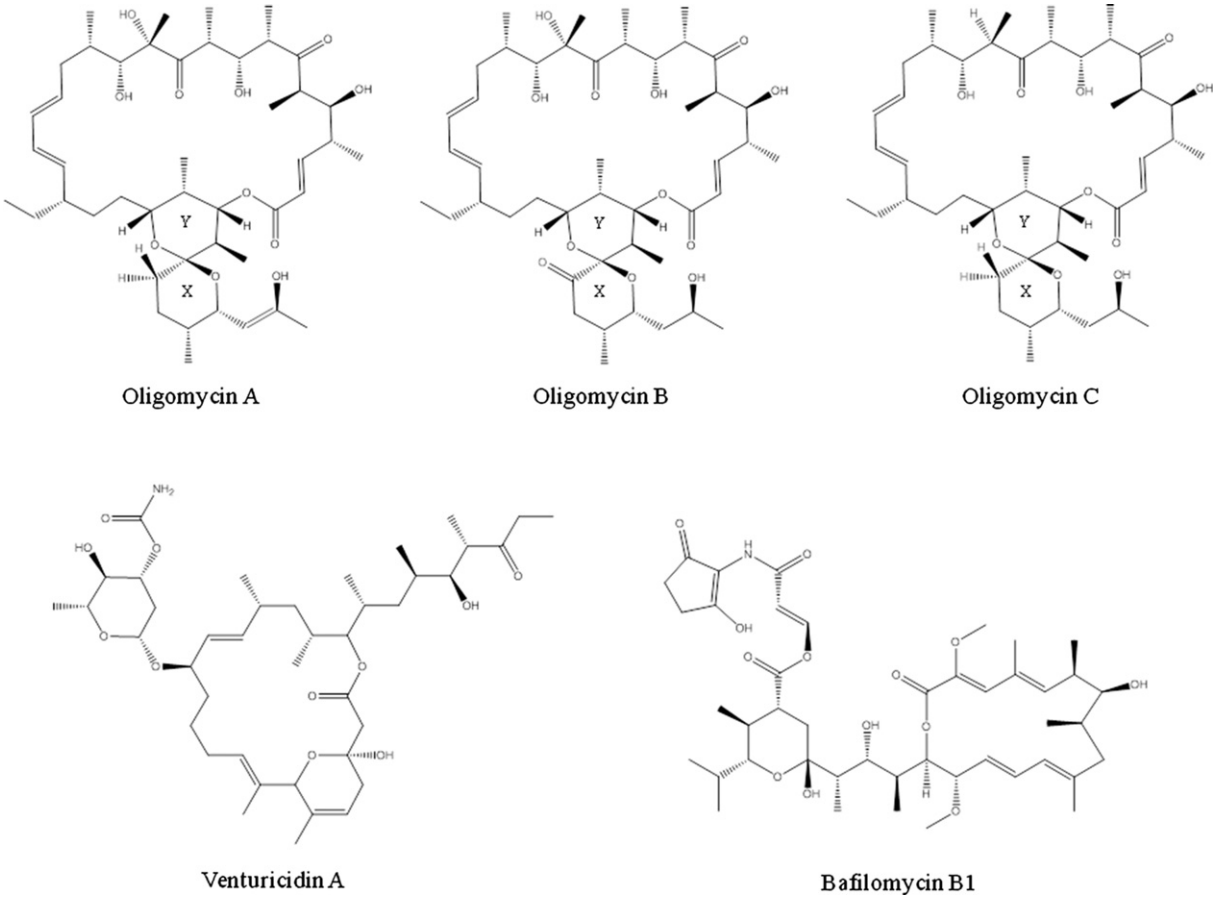

Fig. 9. Structures of oligomycins A, B and C, venturicidin A and bafilomycin B1. The structural differences among oligomycins A, B, and C are highlighted in red.

(Glu59) for protons of C-terminal α-helices of the hairpin structure of *c* subunits, shields the carboxyl access to the aqueous environment of the proton half channel. OLIG binding would not affect the *c*-ring backbone conformation. Conversely, the side chains from Leu63 of *c1* and Phe64 of *c2* subunit would rotate to accommodate between two adjacent C-terminal α-helices the propanol residue linked to the spiro pyranose sugar rings. This conformational change would allow OLIG to bind to the α-helical N-terminus of the *c1* subunit. As far as we are aware, OLIG binding to the *c*-ring seems to involve both hydrophilic and hydrophobic interactions, namely a single hydrogen bond between OLIG and Glu59 via a bridging water molecule and many van der Walls interactions involving 7 amino acids of the C-terminal α-helix, 1 amino acid of the N-terminal α-helix of *c1* subunit and probably 5 amino acids of the C-terminal α-helix of *c2* subunit (Fig. S1). The region which binds OLIG [11] and VENT [29] is localized at the level of the transmembrane domain. Similarly, BAF binds to the transmembrane domain of the V-ATPase [12] which both in eukaryotes and prokaryotes shows strong homologies to F_O [13]. All these macrolide compounds, by binding to specific amino acid residues on two adjacent *c* subunits, block ionic translocation by hampering the torque generation which is essential for the enzyme machinery [30]. This mechanism is fully consistent with the synergistic inhibition kinetics by binary mixtures of macrolides pointed out in the present work (Fig. 3). Accordingly, macrolide binary mixtures resulted into a more striking inhibition than that produced by each individual compound, due to the formation of the quaternary ESI_1I_2 complex. As shown by the equilibrium reactions for the uncompetitive F_1F_O-ATPase inhibition by two different macrolides (I_1 and I_2) which can both bind to the enzyme–substrate complex (Fig. 4), the ESI_1I_2 complex stability is favored by any decrease in $\alpha K'i$ values. A number of factors such as hydrophobic, hydrophilic, ion-dipole and inter-dipole bonds, as well as steric hindrances and protein-conformational changes, may affect the mutual interactions between I_1 and I_2 in the formed ESI_1I_2 complex [31]. On considering α values, it is clear that the three inhibitors tested did not behave the same way. Accordingly, while OLIG and VENT bind independently from each other to yield the quaternary complex, BAF and VENT as well as OLIG and BAF interact with each other in facilitating the binding of the co-present inhibitor, thus producing a striking synergistic inhibitory effect (Fig. 5). The formation of a quaternary complex strongly suggests that each macrolide among the three related compounds tested binds to its specific site on the *ES* complex. On these bases, it is tempting to speculate that each macrolide requires a different amino acid combination to bind to F_O. Since BAF, which was apparently the less powerful inhibitor, enhanced the enzyme inhibition by either OLIG or VENT and positively interacted with both macrolides, BAF binding may trigger changes within F_O. Accordingly, these changes could somehow increase the availability/reactivity of the amino acid side-chains required to bind the co-present macrolide. However, the possible involvement of concentration effects, due to the much higher BAF dose employed, cannot be completely ruled out. As far as we are aware the number of oligomycin or other macrolide molecules which can simultaneously bind to F_O under physiological conditions is still undefined. Even if oligomycin was long believed to bind to F_O in a 1:1 stoichiometry, at present it seems clear that the *c*-ring not only may bind various oligomycin molecules by α-helices of adjacent *c*-subunits, as shown by crystallographic studies [11,15], but also multiple macrolide molecules which share their binding region. Some points remain to be clarified, for instance if the shared region embraces non-adjacent *c*-subunits within the same *c*-ring and if the macrolide-specific binding sites are at least partially overlapping. Macrolide crowding within the shared binding region could also be somehow prevented by steric hindrances. The *c*-ring constitution, namely the number of *c*-subunits containing suitable amino acidic anchors, may play a role in macrolide inhibition once assessed that the number of inhibitor molecules bound to F_O modulates the inhibition extent. The non-additive (synergistic) inhibition suggests that the inhibition potency is primarily ruled by the interaction between different macrolides. Even if multiple inhibitor molecules can accommodate within the *c*-ring, the binding of a single macrolide molecule to its specific site is likely to be sufficient to promote structural distortions which block proton flux within F_O [11]. Interestingly, macrolides such as BAF, although per se poorly effective on the ATP synthase, may favor the binding of other macrolides, thus enhancing inhibition.

The decrease in the mitochondrial ATPase sensitivity to macrolides by TBT is another open question. In the present study, the dose-dependent effect of TBT, first described for OLIG in mollusks [19], was found to extend to VENT and, even if to a less pronounced extent, to BAF (Fig. 6). The TBT-driven ATPase refractoriness to OLIG, not associated with intrinsic enzyme uncoupling, was ascribed to TBT binding to a low-affinity site for TBT on F_O [32]. TBT easily binds to sulfhydryl groups of proteins [33], specifically interacts with those biomolecules that play an essential role in cellular redox signaling [34] and significantly decreases free –SH groups in mitochondria (Fig. 8). On these bases, the enzyme desensitization to OLIG is likely to be ascribed to the onset of covalent tin–sulphur bonds between the organotin toxicant and the enzyme. The TBT binding would modify the oligomycin-blocked F_O conformation leading to proton translocation recovery [15,35,36]. The similar TBT-driven F_1F_O-ATPase refractoriness to OLIG, VENT and BAF strongly suggests that TBT binding somehow modifies an enzyme region which similarly hosts and binds the three polyketide antibiotics under study. The complete removal of the enzyme desensitization to OLIG and VENT by DTE, which reduces thiol groups (Fig. 7), is fully consistent with the hypothesized thiol involvement in the TBT binding leading to the enzyme desensitization. However, since DTE was apparently less efficient in restoring the enzyme sensitivity to BAF, it seems likely that the steric hindrance and/or the hydrophobicity of TBT butyl chains [35] may also play a role in modifying the protein conformation. In this case, these TBT features would cooperate with thiol oxidation to yield the conformational change which destabilizes the *ESI* complex. Taken as a whole, the present data shoulder the hypothesis that OLIG, VENT and BAF bind to a common F_O region, which can be envisaged as a sort of binding pocket, but specifically interact with selectively targeted amino acids. In other words, the macrolides under study would bind to different sites without preventing, and in the case of BAF even favoring, the binding of other structurally related compounds, thus leading to a synergistically enhanced enzyme inhibition. In all cases TBT, by binding to enzyme thiols and causing their oxidation, would act as a destabilizer of the *ESI* complex, resulting into the enzyme desensitization to macrolides.

Assumed that TBT binds to thiols by a covalent tin–sulphur bond, one wonders which cysteine residue could be involved in the putative TBT binding. Strong clues coming from the finding that Cys65 substitution with serine confers oligomycin resistance to *Saccharomyces cerevisisae* mutants [37], indicate this amino acid residue on the C-terminal α-helix of the *c* subunit as the most likely candidate. Since apparently cysteine thiols must be in the reduced state to confer OLIG susceptibility, TBT by binding to cysteine sulphur would cause dehydrogenation, alter the interhelical packing of protomers and destabilize the interactions between macrolides and *c* subunits (Movie S1).

A decreased oligomycin sensitivity has already been associated with defective ATP synthases under various pathological conditions [15] whose main symptoms are shown in high energy demanding tissues such as the nervous tissue, muscle and heart. In human neuromuscular diseases, such as NARP (*N*europathy *A*taxia *R*etinitis *P*igmentosa) and MILS (*M*aternally *I*nherited *L*eigh's *S*yndrome), the impaired function of F_1F_O-ATPase was found to be associated with transitions or transversions in codons of the mtDNA ATPase 6 gene [38] which encodes an essential subunit in proton translocation.

Interestingly, the amino acid residues of *c* subunits are 100% conserved among mammals, including humans, and highly conserved

from yeasts to mammals, however they strongly differ from the bacterial homologs [1,8,11,36]. Since the *c*-subunit amino acid difference between bacteria and mammalian mitochondria appears to be tightly related to the sensitivity to macrolide antibiotics, the identification of the crucial amino acids involved in macrolide binding could be helpful to address the synthesis/discovery of antimicrobial drugs. Accordingly, the information coming from studies on drug/ATP synthase interactions may be widely exploited in the development of therapeutic strategies to counteract mycobacterial diseases, mitochondrial dysfunctions and cancer [26,39].

The present data, which are consistent with the existence of a common macrolide binding region on F_O [11] in which each out of the three macrolides tested would selectively bind to its specific site, strongly suggest a putative mechanism for the overall macrolide F_1F_O-ATPase desensitization by TBT. Additionally, the sensitivity to OLIG and related compounds can be taken as a symptom of the coupled function between the proton-driven motor F_O and the ATP-driven motor F_1 [40]. Therefore, as a corollary, the understanding of the mechanistic basis of the F_1F_O-ATPase desensitization to polyketide antibiotics may provide some insight in the still poorly elucidated mechanism by which the transmembrane proton-motive force generates the *c*-ring rotation.

Supplementary data to this article can be found online at http://dx.doi.org/10.1016/j.bbagen.2014.01.008.

Acknowledgement

This work was financed by the University of Bologna, Italy (RFO grant).

References

[1] F. Dabbeni-Sala, A.K. Rai, G. Lippe, F_OF_1 ATPsynthase: a fascinating challenge for proteomics, in: T.K. Man (Ed.), Proteomics-Human Diseases and Protein Functions, InTech, China, 2012, pp. 161–188, (www.intechopen.com).
[2] J.E. Walker, The ATP synthase: the understood, the uncertain and the unknown, Biochem. Soc. Trans. 41 (2013) 1–16.
[3] R. Iino, H. Noji, Operation mechanism of F_OF_1-adenosine triphosphate synthase revealed by its structure and dynamics, IUBMB Life 65 (2013) 238–246.
[4] H.A. Lardy, D. Johnson, W.C. McMurray, Antibiotics as tools for metabolic studies. I. A survey of toxic antibiotics in respiratory, phosphorylative and glycolytic systems, Arch. Biochem. Biophys. 78 (1958) 587–597.
[5] P.W. Yang, M.G. Li, J.Y. Zhao, M.Z. Zhu, H. Shang, J.R. Li, X.L. Cui, R. Huang, M.C. Wen, Oligonycins A and C, major secondary metabolites isolated from the newly isolated strain *Streptomyces diastaticus*, Folia Microbiol. (Praha) 55 (2010) 10–16.
[6] D.S. Perlin, L.R. Latchney, A.E. Senior, Inhibition of Escherichia coli H^+-ATPase by venturicidin, oligomycin and ossamycin, Biochim. Biophys. Acta 807 (1985) 238–244.
[7] A.R. Salomon, Y. Zhang, H. Seto, C. Khosla, Structure-activity relationships within a family of selectively cytotoxic macrolide natural products, Org. Lett. 3 (2001) 57–59.
[8] I.N. Watt, M.G. Montgomery, M.J. Runswick, A.G. Leslie, J.E. Walker, Bioenergetic cost of making an adenosine triphosphate molecule in animal mitochondria, Proc. Natl. Acad. Sci. U. S. A. 107 (2010) 16823–16827.
[9] S. Nesci, V. Ventrella, F. Trombetti, M. Pirini, A. Pagliarani, Mussel and mammalian ATP synthase share the same bioenergetic cost of ATP, J. Bioenerg. Biomembr. 45 (2013) 289–300.
[10] D. Pogoryelov, A. Krah, J.D. Langer, Ö. Yildiz, J.D. Faraldo-Gómez, T. Meier, Microscopic rotary mechanism of ion translocation in the F(o) complex of ATP synthases, Nat. Chem. Biol. 6 (2010) 891–899.
[11] J. Symersky, D. Osowski, D.E. Walters, D.M. Mueller, Oligomycin frames a common drug-binding site in the ATP synthase, Proc. Natl. Acad. Sci. U. S. A. 109 (2012) 13961–13965.
[12] B.J. Bowman, E.J. Bowman, Mutations in subunit *c* of the vacuolar ATPase confer resistance to bafilomycin and identify a conserved antibiotic binding site, J. Biol. Chem. 277 (2002) 3965–3972.
[13] B.J. Bowman, M.E. McCall, R. Baertsh, E.J. Bowman, A model for the proteolipid ring and bafilomycin/concanamycin-binding site in the vacuolar ATPase of *Neurospora crassa*, J. Biol. Chem. 281 (2006) 31885–31893.
[14] A.Y. Mulkidjanian, M.Y. Galperin, E.V. Koonin, Co-evolution of primordial membranes and membrane proteins, Trends Biochem. Sci. 34 (2009) 206–215.
[15] A. Pagliarani, S. Nesci, V. Ventrella, Modifiers of the oligomycin sensitivity of the mitochondrial F_1F_O-ATPase, Mitochondrion 13 (2013) 312–319.
[16] F. Pellotti, G. Lenaz, Isolation and subfractionation of mitochondria from animal cells and tissue culture lines, Methods Cell Biol. 80 (2007) 3–44.
[17] M.M. Bradford, A rapid and sensitive method for the quantitation of microgram quantities of protein utilizing the principle of protein-dye binding, Anal. Biochem. 72 (1976) 248–254.
[18] C.G. Fiske, Y. Subbarow, The colorimetric determination of phosphorus, J. Biol. Chem. 66 (1925) 375–400.
[19] S. Nesci, V. Ventrella, F. Trombetti, M. Pirini, A. Pagliarani, Multi-site TBT binding skews the inhibition of oligomycin on the mitochondrial Mg-ATPase in *Mytilus galloprovincialis*, Biochimie 93 (2011) 1157–1164.
[20] M. Dixon, E.C. Webb, Enzymes, third ed. Academic Press, New York, 1979.
[21] A. Cornish-Bowden, A simple graphical method for determining the inhibition constants of mixed, uncompetitive and non-competitive inhibitors, Biochem. J. 137 (1974) 143–144.
[22] I.H. Segel, Enzyme Kinetics, John Wiley and Sons, Inc., New York, 1975.
[23] G.L. Ellman, Tissue sulfhydryl groups, Arch. Biochem. Biophys. 82 (1959) 70–77.
[24] C.K. Riener, G. Kada, H.J. Gruber, Quick measurement of protein sulphydryls with Ellman's reagent and with 4.4′-dithiopyridine, Anal. Bioanal. Chem. 373 (2002) 266–276.
[25] S. Nesci, V. Ventrella, F. Trombetti, M. Pirini, A. Pagliarani, Tributyltin (TBT) and mitochondrial respiration in mussel digestive gland, Toxicol. In Vitro 25 (2011) 951–959.
[26] Z. Ahmad, F. Okafor, S. Azim, T.F. Laughlin, ATP synthase: a molecular therapeutic drug target for antimicrobial and antitumor peptides, Curr. Med. Chem. 20 (2013) 1956–1973.
[27] P. Boyer, The ATP synthase—a splendid molecular machine, Annu. Rev. Biochem. 66 (1997) 717–749.
[28] D. Goodsell, ATP Synthase Molecule of the Month, 2005., http://dx.doi.org/10.2210/rcsb_pdb/mom_2005_12.
[29] P. Nagley, R.M. Hall, B.G. Ooi, Amino acid substitutions in mitochondrial ATPase subunit 9 of *Saccharomyces cerevisiae* leading to oligomycin or venturicidin resistance, FEBS Lett. 195 (1986) 159–163.
[30] W. Junge, H. Sielaff, S. Engelbrecht, Torque generation and elastic power transmission in the rotary F(O)F(1)-ATPase, Nature 459 (2009) 364–370.
[31] T. Yonetani, The Yonetani-Theorell graphical method for examining overlapping subsites of enzyme active centers, Methods Enzymol. 87 (1982) 500–509.
[32] S. Nesci, V. Ventrella, F. Trombetti, M. Pirini, A. Pagliarani, Tri-*n*-butyltin binding to a low-affinity site decreases the F_1F_O-ATPase sensitivity to oligomycin in mussel mitochondria, Appl. Organomet. Chem. 26 (2012) 593–599.
[33] A. Pagliarani, S. Nesci, F. Trombetti, V. Ventrella, Organotin effects on membrane-bound ATPase activities, in: H.F. Chin (Ed.), Organometallic Compounds: Preparation, Structure and Properties, Nova Science Publishers Inc., New York, 2010, pp. 225–253.
[34] M.P. Murphy, Modulating mitochondrial intracellular location as a redox signal, Sci. Signal. 5 (2012) pe39.
[35] S. Nesci, V. Ventrella, F. Trombetti, M. Pirini, A. Pagliarani, Tributyltin-driven enhancement of the DCCD insensitive Mg-ATPase activity in mussel digestive gland mitochondria, Biochimie 94 (2012) 727–733.
[36] S. Nesci, V. Ventrella, F. Trombetti, M. Pirini, A. Pagliarani, The mitochondrial F1FO-ATPase desensitization to oligomycin is due to thiol oxidation, Biochimie 97 (2014) 128–137, http://dx.doi.org/10.1016/j.biochi.2013.10.002.
[37] W. Sebald, E. Wachter, A. Tzagoloff, Identification of amino acid substitutions in the dicyclohexylcarbodiimide-binding subunit of the mitochondrial ATPase complex from oligomycin-resistant mutants of *Saccharomyces cerevisiae*, Eur. J. Biochem. 100 (1979) 599–607.
[38] E.A. Schon, S. Santra, F. Pallotti, M.E. Girvin, Pathogenesis of primary defects in mitochondrial ATP synthesis, Semin. Cell Dev. Biol. 12 (2001) 441–448.
[39] J.A. Johnson, M. Ogbi, Targeting the F1Fo ATP synthase: modulation of the body's powerhouse and its implications for human disease, Curr. Med. Chem. 18 (2011) 4684–4714.
[40] R.J. Devenish, M. Prescott, G.M. Boyle, P. Nagley, The oligomycin axis of mitochondrial ATP synthase: OSCP and the proton channel, J. Bioenerg. Biomembr. 32 (2000) 507–515.